PHASE STRESS DETERMINATION AND SIMULATION FOR AZ COMPOSITE HAVING STRESS GRADIENT IN OR THOPEDIC APPLICATIONS

TÍNH TOÁN MÔ PHỎNG ỨNG SUẤT PHA CHO VẬT LIỆU COMPOSITE AZ CÓ GRADIENT ỨNG SUẤT TRONG LÃNH VỰC CHỈNH HÌNH

Le Chi Cuong, Chau Thi Anh Tuyet
Ho Chi Minh City University of Technology and Education

Received 13/10/2015, Peer reviewed 30/12/2015, Accepted for publication 05/01/2016.

ABSTRACT

The X-ray stress of dual-phase composite AZ is determined from X-ray elastic constants by using Reuss, Voigt and Eshelby–Kroner models. The simulated result showed that the compound XEC in the Reuss model is independent of the volume composition of inclusion Al_2O_3 and it is valid for low inclusion composition. The Voigt and Eshelby-Kroner models gave closed stress values to the experimental result, while they are constant for the Reuss model.

Keywords: *X-ray Elastic Constants (XEC), Alumina-Zirconia (AZ) composite, Stress Gradient.*

TÓM TẮT

Ứng suất của vật liệu composite hai pha AZ bằng nhiễu xạ X–quang được xác định dựa trên ba mô hình Reuss, Voigt và Eshelby–Kroner. Kết quả tính toán cho thấy: hằng số XEC được xác định bằng mô hình Reuss không phụ thuộc vào tỉ lệ thể tích pha liên kết trong trường hợp tỉ lệ thể tích pha Al_2O_3 là rất nhỏ. Mô hình Voigt và Eshelby–Kroner cho kết quả tính toán ứng suất gần nhau và với giá trị thực nghiệm hơn so với mô hình Reuss.

Từ khóa: *Hằng số đàn hồi tia X (XEC), Vật liệu composite Alumina-Zirconia, Gradient Ứng suất.*

1. INTRODUCTION

Alumina (Al_2O_3) is a material having many advanced properties, such as chemical and heat resistance, and is used in mechanical and bio-medical areas. To enhance the strength and toughness, zirconia (ZrO_2) powder is mixed into alumina as a matrix in a controlled composition to create alumina-zirconia composite Al_2O_3/ZrO_2 (AZ) [1,2]. Depending on the purpose, the composition is between 20% to 60% in volume (commonly 20% to 50%). Many researches are trying to determine the phase stress of AZ by using many X-ray characteristics for various azimuth measurements; however, this is timely and significantly reduces the measurement accuracy [3,4]. This research introduces the computation of stress and X-ray elastic constants (XEC) of isotropic AZ composite having stress gradient.

Table 1. *Young modulus E and Poisson ratio v of AZ composite*[1]

Materials	Volume Al_2O_3	*E*, GPa	v
Al_2O_3	-	423	0.224
ZrO_2	-	169	0.314
Al_2O_3/ZrO_2	27,3%	241	0,283

2. STRAIN-STRESS RELATION

Let us consider coordinate systems the surface layer of specimen having double phases α and γ as shown in Fig. 1. S_i is the specimen system, in which S_1, S_2 are on the surface, and S_3 is in the normal direction. L_i is the laboratory system, where L_3 ($L_{\varphi\psi}$) is perpendicular to the diffraction plane (hkl). L_2 is on the surface plane and makes an angle φ

to S_1. The strain in the L_3 is determined from the transformation matrix as [5]:

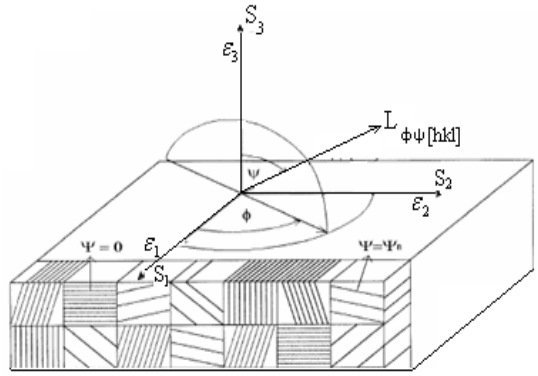

***Fig. 1**. Coordinate system in the surface layer of double phase specimen.*

$$\left(\varepsilon_3^{'}\right)_{\varphi\psi} = \frac{1}{2}S_2\left(\sigma_1\cos^2\varphi + \sigma_{12}\sin 2\varphi + \sigma_2\sin^2\varphi\right)\sin^2\psi + \frac{1}{2}S_2\left(\sigma_3\right) + S_1\left(\sigma_1+\sigma_2+\sigma_3\right) + \frac{1}{2}S_2\left(\sigma_{13}\cos\varphi + \sigma_{23}\sin\varphi\right)\sin 2\psi \quad (1)$$

The average macro stress σ_i in the irradiated area is determined from the phase stresses of phases α and β and the phase ratio V_f as [2,6]:

$$\left\langle\sigma_i\right\rangle_\alpha V_f + \left\langle\sigma_i\right\rangle_\beta\left(1-V_f\right) = \sigma_i \quad (2)$$

where

The phase micro stress is determined as

$$\left\langle\sigma_i'\right\rangle_{pha} = \left\langle\sigma_i\right\rangle_{pha} - \sigma_i \quad (3)$$

3. PHASE X-RAY ELASTIC CONSTANT (XEC)

For single phase material, the strain in the 11 direction (φ=0°,ψ) is:

$$\varepsilon_{\varphi\psi} = \frac{1}{2}S_2\left(\sigma_1-\sigma_3\right)\sin^2\psi + \frac{1}{2}S_2\sigma_3 + S_1\left(\sigma_1+\sigma_2+\sigma_3\right) \quad (4)$$

where the indices of stresses 1, 2 and 3 denote the indices 11, 22 and 33. The diffraction angles $\theta_{0,\psi}$ and $\theta_{90,\psi}$ in the directions (φ=0°,ψ) and (φ=90°,ψ) are respectively determined as:

$$2\theta_{0,\psi} = 2\theta_0 - \tan\theta_0 S_2\left(\sigma_1-\sigma_3\right)\sin^2\psi - \tan\theta_0 S_2\sigma_3 - 2S_1\tan\theta_0\left(\sigma_1+\sigma_2+\sigma_3\right) \quad (5)$$

$$2\theta_{\varphi=90^0,\psi} = 2\theta_0 - \tan\theta_0 S_2\left(\sigma_2-\sigma_3\right)\sin^2\psi - \tan\theta_0 S_2\sigma_3 - 2S_1\tan\theta_0\left(\sigma_1+\sigma_2+\sigma_3\right) \quad (6)$$

From Eqs.(4) and (6), XEC is determined as:

$$S_1 = -\frac{\cot\theta_0}{2}\frac{\partial\left(2\theta_{0\psi=0}\right)}{\partial\sigma_A}$$

$$\frac{1}{2}S_2 = -\frac{\cot\theta_0}{2}\frac{\partial}{\partial\sigma_A}\left(\frac{\partial 2\theta_{0\psi}}{\partial\sin^2\psi}\right) \quad (7)$$

where σ_A is the applied stress, determined from the strain gauge experimentally.

In the multiphase material, due to the interaction between phases, XEC of each phase is different from those for the single phase, and it is called compound XEC, denoted as upper indices "C".

$$\varepsilon_{ij}^{\text{pha}} = \frac{1}{2}S_2^{C,\text{pha}}\sigma_j - \delta_j S_1^{C,\text{pha}}\sigma_j \quad (8)$$

where $S_1^{C,\text{pha}}$ and $0.5S_2^{C,\text{pha}}$ are XEC of phase in the matrix; δ_{ij} are the Kronerker's delta, determined as δ_{ij}= 0 if $i \neq j$ and δ_{ij}= 1 if $i = j$. From Eq.(7) the phase XEC in the matrix can be determined as:

$$\frac{1}{2}S_2^{C,\text{pha}} = -\frac{\cot\theta_0^{\text{pha}}}{2}\frac{\partial}{\partial\sigma_A}\left(\frac{\partial 2\theta_{0\psi}^{\text{pha}}}{\partial\sin^2\psi}\right)$$

$$S_1^{C,\text{pha}} = -\frac{\cot\theta_0^{\text{pha}}}{2}\frac{\partial\left(2\theta_{0\psi=0}^{\text{pha}}\right)}{\partial\sigma_A} \quad (9)$$

Substituting Eqs.(5,6) into (9), the relation ibetween the XEC in the matrix and XEC of single phase is determined as:

$$\frac{1}{2}S_2^{C,\text{pha}} = \frac{1}{2}S_2\frac{\partial}{\partial\sigma_A}\left(\sigma_1-\sigma_3\right)$$

$$S_1^{C,\text{pha}} = \frac{1}{2}S_2\frac{\partial\sigma_3}{\partial\sigma_A} + S_1\frac{\partial}{\partial\sigma_A}\left(\sigma_1+\sigma_2+\sigma_3\right) \quad (10)$$

However, the determination of compound XEC from the experiment as shown in Eq. (9) is timely and often generates inaccuracy. In the case of the measurement accuracy in not required, the XEC can be

estimated from the theory by using three models of Reuss, Voigt and Eshelby–Kroner.

3.1. Reuss model

In the Reuss model, the stresses are constant for all phases, and the compound XEC is independent of the other phase existence [5,8]. The XECs of phases Al_2O_3 and ZrO_2 are given in Table 2[7,9].

Table 2. *XECs of phases Al_2O_3 and ZrO_2*

Al_2O_3	ZrO_2
$S_1^{C,I}=-\frac{\nu^I}{E^I}=-0{,}53\times10^{-6}\text{MPa}^{-1}$	$S_1^{C,M}=-\frac{\nu^M}{E^M}=-1{,}9\times10^{-6}\text{MPa}^{-1}$
$\frac{1}{2}S_2^{C,I}=\frac{1+\nu^I}{E^I}=2{,}89\times10^{-6}\text{MPa}^{-1}$	$\frac{1}{2}S_2^{C,M}=\frac{1+\nu^M}{E^M}=7{,}8\times10^{-6}\text{MPa}^{-1}$

3.2. Voigt model

The Voigt model accepts that the phase strains are constant [5,8]. The Lame's constants and shearing modulus of individual phases in the compound are

$$\lambda^{I,M}=\frac{\nu^{I,M}E^{I,M}}{\left(1+\nu^{I,M}\right)\left(1-2\nu^{I,M}\right)},\quad \lambda^C=V_f\lambda^I+\left(1-V_f\right)\lambda^M \tag{11}$$

$$\mu^{I,M}=\frac{E^{I,M}}{2\left(1+\nu^{I,M}\right)},\quad \mu^C=V_f\mu^I+\left(1-V_f\right)\mu^M \tag{12}$$

Substituting the Young's modulus and Poisson ratios into Eq.(11), we have

λ^I = 140GPa, λM = 109GPa, λC = 117GPa

μ^I = 173GPa, μ^M = 64,3GPa, μ^C = 94GPa

Therefore the Young's modulus and Poisson ratio of compound are:

$$E^{C,V}=\frac{\left(3\lambda^C+2\mu^C\right)\mu^C}{\lambda^C+\mu^C}=240\text{GPa} \tag{13}$$

$$\nu^{C,V}=\frac{\lambda^C}{2\left(\lambda^C+\mu^C\right)}=0{,}278 \tag{14}$$

Therefore the compound XECs in the Voigt model are:

$$S_1^{C,I}=S_1^{C,M}=S_1^C=\frac{1}{2}S_2^I\frac{E^I}{E^{C,V}}\frac{\nu^I-\nu^{C,V}}{\left(1+\nu^I\right)\left(1-2\nu^I\right)}$$

$$+S_1^I\frac{E^I}{E^{C,V}}\frac{1-2\nu^{C,V}}{1-2\nu^I}=-1.156\times10^{-6}\text{MPa}^{-1}$$

$$=-1,2\times10^{-6}\text{MPa}^{-1}$$

$$\frac{1}{2}S_2^{C,I}=\frac{1}{2}S_2^{C,M}=\frac{1}{2}S_2^C$$

$$=\frac{1}{2}S_2^I\frac{E^I}{E^{C,V}}\frac{1+\nu^{C,V}}{1+\nu^I}=5.3\times10^{-6}\text{MPa}^{-1}$$

For the multiphase materials, the Lame constant is determined from the individual phases are [6]

$$\lambda^C=V_1\lambda^1+V_2\lambda^2+...V_n\lambda^n$$

Similarly, the shearing modulus μ^C, Poisson ratio ν^C and XEC of the compound can also be determined.

3.3. Eshelby–Kroner model

In the self-consistence theory of Eshelby-Kroner, the compression modulus k^C and shearing modulus G^C are determined as [5,8]

$$k^C=k^M+\frac{V_f\left(k^I-k^M\right)\left(3k^C+4G^C\right)}{3k^I+4G^I} \tag{15}$$

$$G^C=G^M+\frac{5V_fG^C\left(G^I-G^M\right)\left(3k^C+4G^C\right)}{8G^{C^2}+G^C\left(9k^C+12G^I\right)+6k^CG^I} \tag{16}$$

where $k=\frac{E}{3(1-2\nu)}$; $\quad G=\frac{E}{2(1+\nu)}$

We obtain $E^{C,E}$ = *255 x 10^3MPa and* $\nu^{C,E}$ = *0,291*

$$S_1^C=-\nu^{C,E}/E^{C,E}=-1.1\times10^{-6}\text{MPa}^{-1}$$

$$\frac{1}{2}S_2^C=(1+\nu^{C,E})/E^{C,E}=5.1\times10^{-6}\text{MPa}^{-1}$$

The similar computation gives the XECs in the Eshelby-Kroner model. Figure 2 shows the XECs from the three models with various phase composition of Al_2O_3. As the Al_2O_3 increases the XEC decreases, showing the increasing hardness of material. The Voigt and Eshelby-Kroner models give the closer XEC to the experimental data in comparison to the Reuss model [10]. This means the Reuss model is valid only for very low Al_2O_3 composition, say less than 5%.

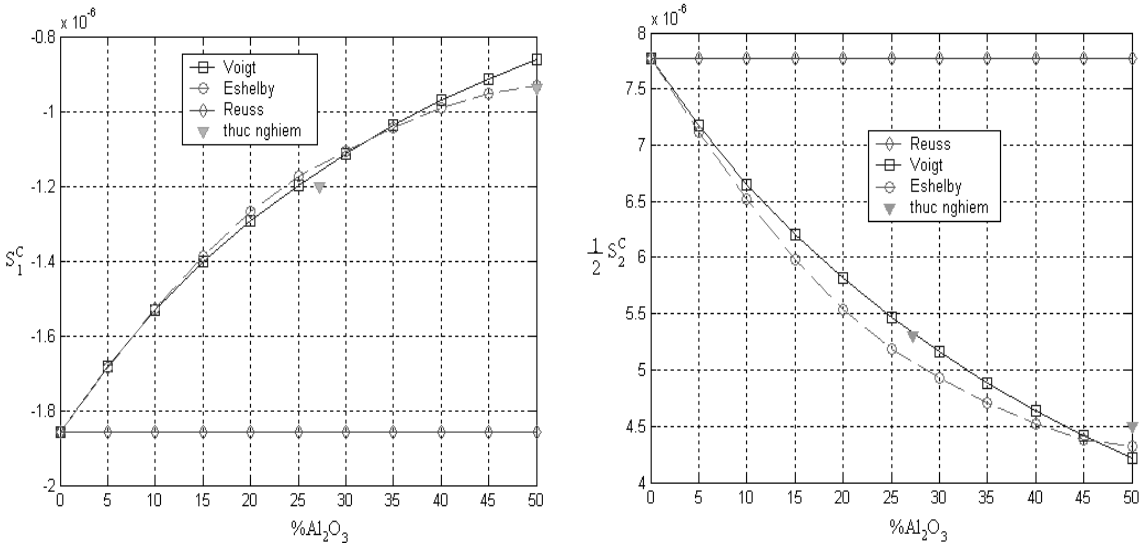

***Fig. 2**. X-ray elastic constants S_1^C and $\frac{1}{2}S_2^C$ with phase ratio of Alumina*

4. PHASE STRESS

4.1. Reuss model

In the Reuss model, phase stresses exactly equal to a loading stresses or residual stresses.

4.2. Voigt model

When a loading stress σ_A is applied to the direction 11, the matrix stress $\langle\sigma_i\rangle_M$ is calculated as [5,6]:

$$\langle\sigma_1\rangle_M = \frac{1}{3}\left(A^V + 2B^V\right)\sigma_A \tag{17}$$

$$\langle\sigma_2\rangle_M = \langle\sigma_3\rangle_M = \frac{1}{3}\left(A^V - B^V\right)\sigma_A \tag{18}$$

where:

$$A^V = \frac{E^M\left(1-2\nu^{C,V}\right)}{E^{C,V}\left(1-2\nu^M\right)} \quad B^V = \frac{E^M\left(1+\nu^{C,V}\right)}{E^{C,V}\left(1+\nu^M\right)}$$

From Eqs.(17) and (18), the normal stress components $\langle\sigma_1\rangle_M, \langle\sigma_2\rangle_M, \langle\sigma_3\rangle_M$ of the matrix ZrO_2, then stress of inclusion can be determined and illustrated as shown in Figs. 3 and 4. As the inclusion composition Al_2O_3 increases, the stresses $\langle\sigma_1\rangle$ decreases and $\langle\sigma_2\rangle$ increases. This simulation may helpful in selection of inclusion/matrix composition to adapt the material usage. Now, the phase micro stress is determined from Eq. (3). The similar results of micro stress and the macro stress for inclusion Alumina and matrix Zirconia can be found as shown in Figs. 5 and 6.

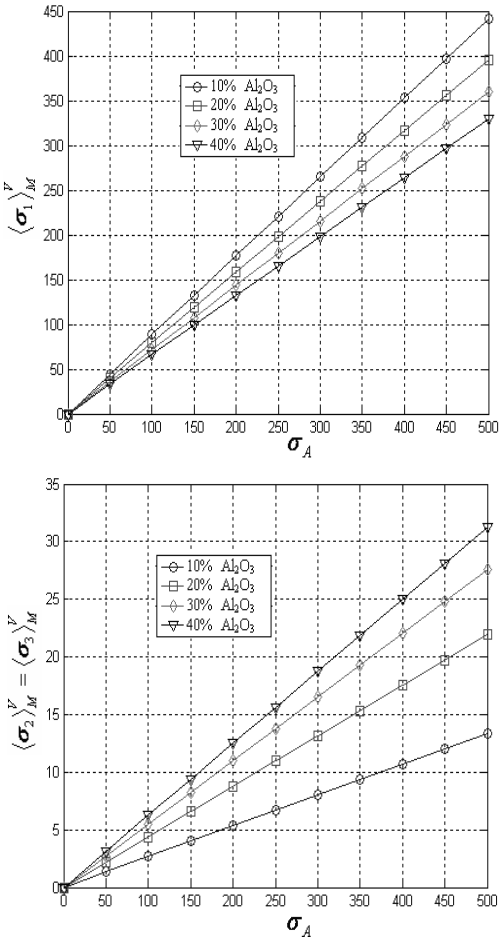

***Fig. 3**. $\langle\sigma_1\rangle_M^V - \sigma_A$ and $\langle\sigma_2\rangle_M^V - \sigma_A$ diagram*

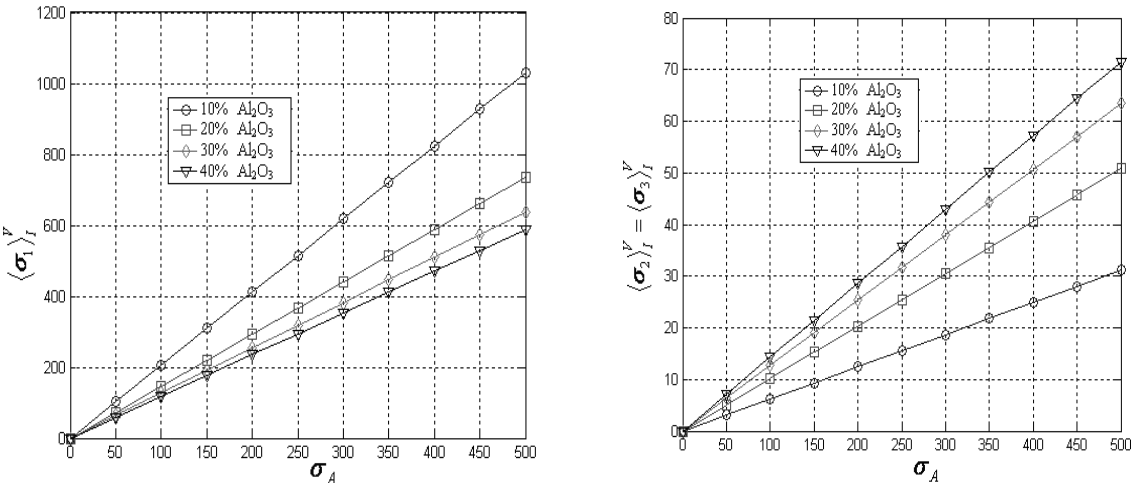

Fig. 4. *$\langle\sigma_1\rangle_I^V - \sigma_A$ and $\langle\sigma_2^I\rangle_I^V - \sigma_A$ diagram*

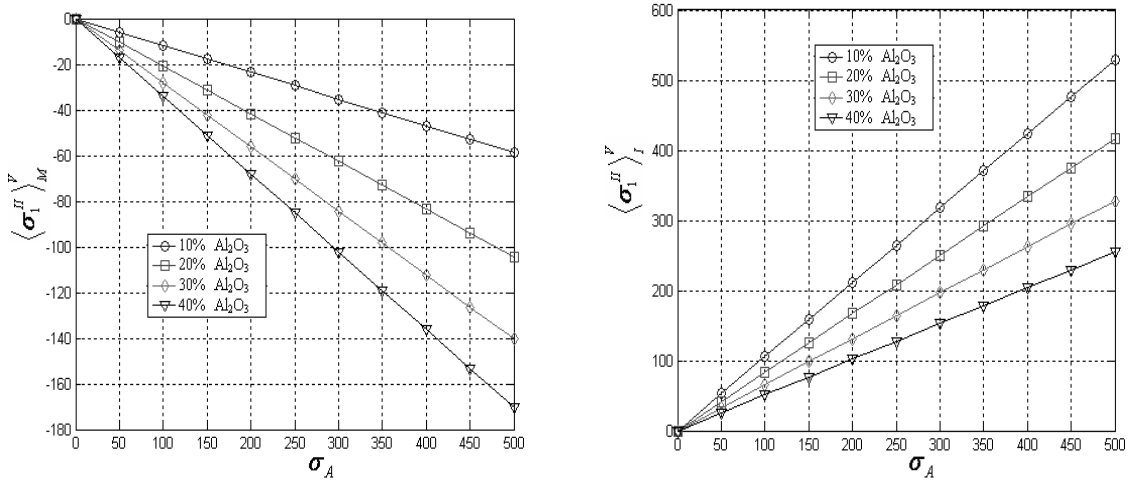

Fig. 5. *$\langle\sigma_1^I\rangle_M^V - \sigma_A$ and $\langle\sigma_1^I\rangle_I^V - \sigma_A$ diagram*

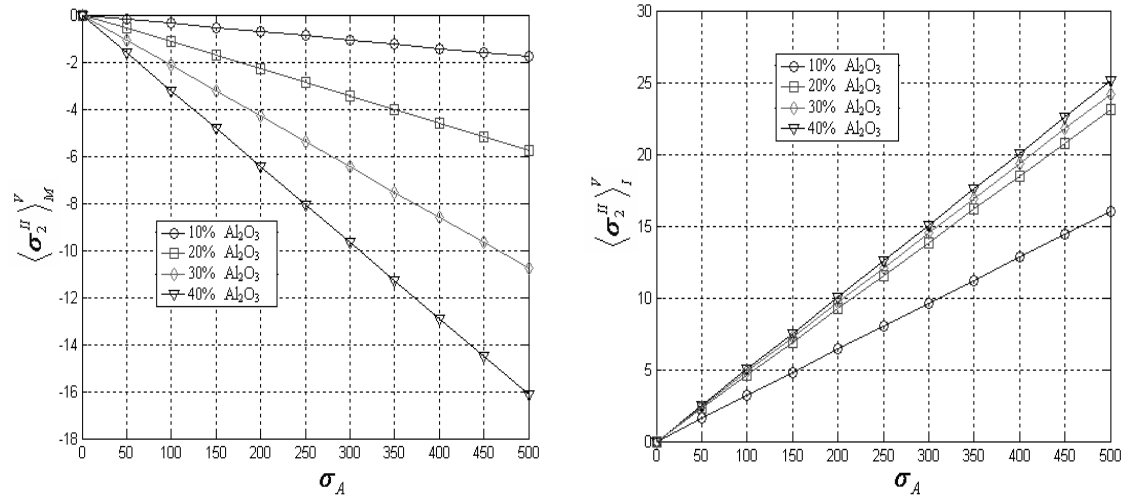

Fig. 6. *$\langle\sigma_2^I\rangle_M^V - \sigma_A$ and $\langle\sigma_2^I\rangle_I^V - \sigma_A$ diagram*

4.3 Eshelby–Kroner model

The computation of stress in the Eshelby-Kroner model is similar to the Voigt model, but for the inclusion Al_2O_3 as[5]

$$\langle\sigma_1\rangle_I = \frac{1}{3}(A+2B)\sigma_A \quad (19)$$

$$\langle\sigma_2\rangle_I = \langle\sigma_3\rangle_I = \frac{1}{3}(A-B)\sigma_A \quad (20)$$

where $A^E = \frac{3(1-\nu^C)E^I}{(1+\nu^C)E^I + 2(1-2\nu^I)E^C}$ and

$$B^E = \frac{5(1-\nu^{C2})E^I}{2(4-5\nu^C)(1+\nu^C)E^I + (7-5\nu^C)(1+\nu^I)E^C}$$

5. $Sin^2\psi$ Diagram Having Stress Gradient

Supposing that the profile of stress gradient in the normal direction is as

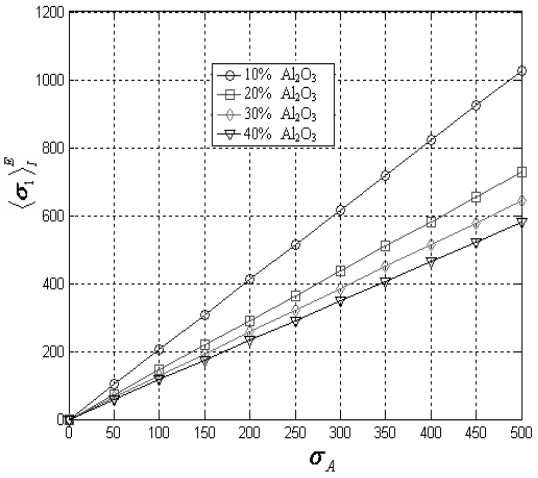

Fig. 7. *$\langle\sigma_1\rangle_I^E - \sigma_A$ relation with Al_2O_3 composition*

$$\sigma_{ij} = \sigma_j^{(z=0)} + a_j z^{n_{ij}} \quad (21)$$

where $\sigma_{ij}(z=0)$ is the stress at the surface layer; a_{ij}, n_{ij} are the constants represented the gradient profile. The stress is defined as the average stress in the X-ray irradiated volume, determined as [5,6]:

$$\langle\sigma_{ij}(\tau)\rangle = \int_0^T \sigma_{ij}(z)e^{\left(-\frac{z}{\tau}\right)}dz \Big/ \int_0^P e^{\left(-\frac{z}{\tau}\right)}dz \quad (22)$$

where T is sample thickness; τ is X-ray penetration depth, $\tau = \frac{\sin^2\theta - \sin^2\psi}{2\mu\sin\theta\cos\psi}$ for Ω-type goniometer, $\tau = (\sin\theta\cos\psi)/2\mu$ for ψ-type goniometer, μ is the linear absorption coefficient. Figure 8 is the relation of the penetration depth with azimuth angle ψ for the matrix ZrO_2

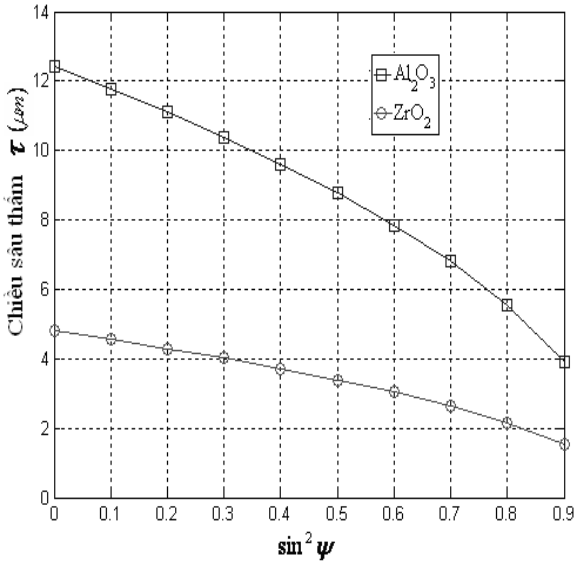

Fig. 8. *Relation of $\tau - \sin^2\psi$ for ψ-type goniometer*

using Cr-Kα, 2θ=133.4°, μ=956cm^{-1} and for inclusion Al_2O_3 using Cr-Kα radiation, 2θ=152°, μ=391cm^{-1}[7]. In fact, the value of σ_{13} is small and we consider the gradient of normal stresses in directions 11 and 33.

5.1. Stress Gradient in the direction 11

For the stress gradient profile in the near-surface layer as shown in Fig. 9, the average stress in the penetration depth τ is determined as[6]

$$\langle\sigma_1(\tau)\rangle = \frac{1}{\tau}\left(\int_0^r \sigma_1(z)e^{-\frac{z}{\tau}}dz + \int_r^b \sigma_1(z)e^{-\frac{z}{\tau}}dz\right)$$
$$= \sigma_1^{(z=0)} + \tau g\left(e^{-\frac{r}{\tau}} - e^{-\frac{b}{\tau}}\right) \quad (23)$$

where $g = \frac{\partial}{\partial z}\sigma(z) = \frac{-\sigma(z=0)}{b-r}$

Supposing $r = 1\mu m$, $b = 5\mu m$, $\sigma_1^{z=0} = -400MPa$, the average stress $\langle\sigma_1(\tau)\rangle$ in the penetration depth depends on the $\sin^2\psi$ direction and is simulated in Fig. 9.

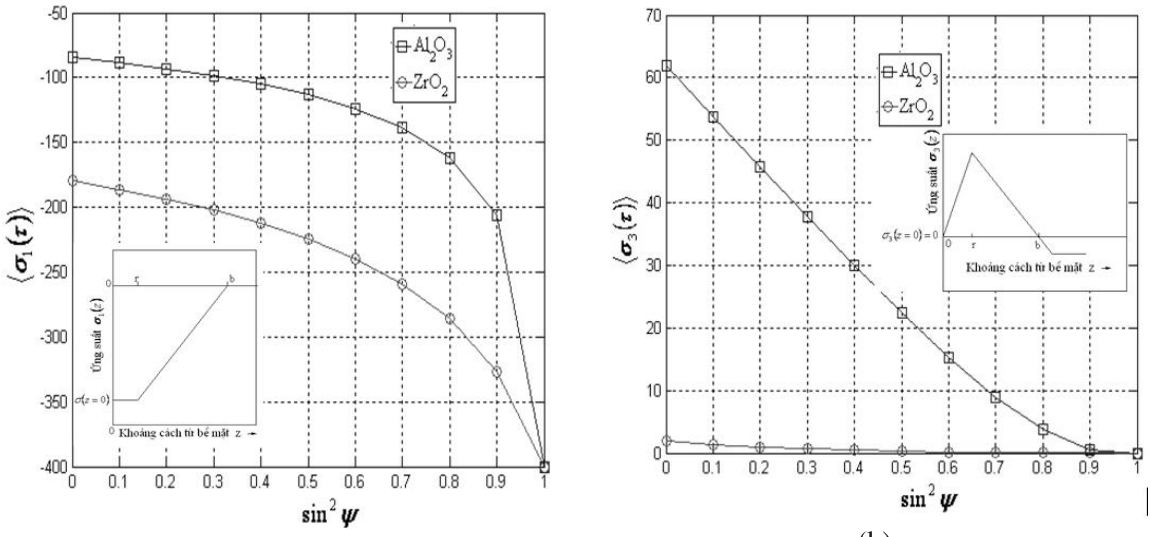

(a) (b)

***Fig. 9**. Stress gradient profile and average stress*

$\langle\sigma_1(\tau)\rangle$ *and* $\langle\sigma_3(\tau)\rangle$ *with* $\sin^2\psi$.

The strain in the direction (φ,ψ) is

$$\langle\varepsilon'_{33}\rangle = \left(\frac{1}{2}S_2\sin^2\psi + S_1\right)\langle\sigma_1(\tau)\rangle$$

$$d_{0,\psi} = d_0 + d_0\left(\frac{1}{2}S_2\sin^2\psi + S_1\right)\left[\sigma_1^{(z=0)} + \tau g\left(e^{-\frac{r}{\tau}} - e^{-\frac{b}{\tau}}\right)\right] \qquad (24)$$

For the matrix ZrO_2, $d_0 = 0{,}509\text{m}$ [7].

5.2. Stress Gradient in the direction 33

Similarly, the average stress $\langle\sigma_3(\tau)\rangle$ for stress gradient profile in Fig. 9(b) can also be determined as

$$\langle\sigma_3(\tau)\rangle = \sigma_3^{(z=0)} + \tau g_1 e^{-\frac{r}{\tau}} - \tau g_2 e^{-\frac{b}{\tau}} \qquad (25)$$

where r = 20μm, b= 220μm
g1(0 z r) = 25MPa/μm,
g2(r z b) = 2,5MPa/μm.

On the other hand, the strain in the direction (φ,ψ) is

$$\langle\varepsilon'_{33}\rangle = \left(\frac{1}{2}S_2 - \frac{1}{2}S_2\sin^2\psi + S_1\right)\langle\sigma_3(\tau)\rangle$$

$$d_{\varphi,\psi} = d_0 + d_0\left(\frac{1}{2}S_2 - \frac{1}{2}S_2\sin^2\psi + S_1\right)\times$$

$$\left[\sigma_3(z=0) + \tau g_1 e^{-\frac{r}{\tau}} - \tau g_2 e^{-\frac{b}{\tau}}\right] \qquad (26)$$

Figure 10 simulates the $\sin^2\psi$ of Zirconia phase having stress gradient in 11 and 33 directions. It is clear that the Voigt and Eshelby-Kroner models give closer results than the Reuss model.

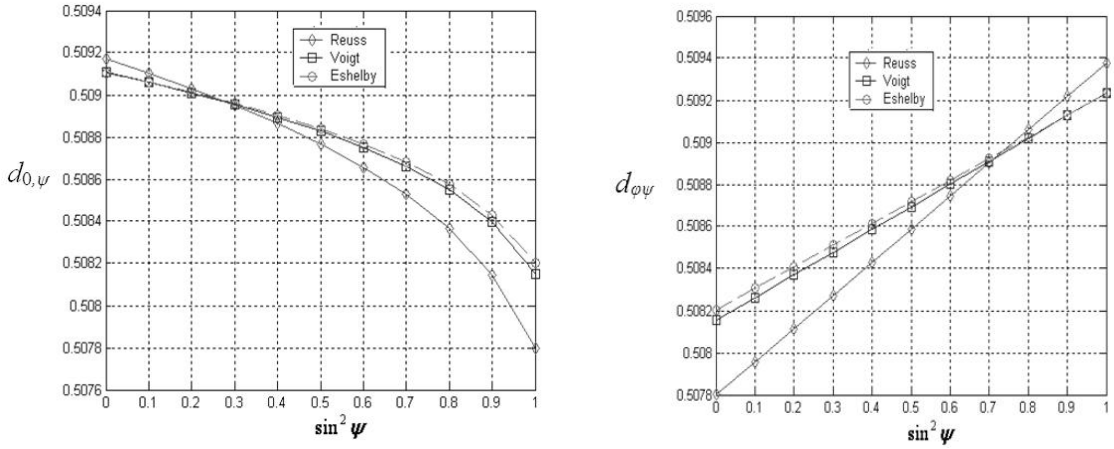

(a) (b)

***Fig. 10.** $Sin^2\psi$ diagram for stress gradient in directions 11 (a) and 33 (b).*

6. CONCLUSION

This paper has computed and simulated the XECs and phase stresses of AZ composite in the case of stress gradient in directions 11 and 33. The simulated $\sin^2\psi$ diagrams may helpful in the case of single measurement without using various X-ray characteristics and many measurements in azimuth angles that affecting the measurement accuracy.

The simulated result can also be useful in selecting appropriate phase composition to adapt requirement of mechanical properties. Further research on anisotropic AZ composite should be done for more accurate analysis.

REFERENCES

[1] B.D.Cullity and S.R.Stock, *Elements of X–ray Diffraction*, Prentice Hall, pp.391-439.

[2] K.Tanaka, S.Kodama and T.Goto, *X–ray Diffraction Studies on The Deformation And Fracture of Solids*, Elsevier Applied Science,1993,pp.1-28.

[3] L.C.Cương, *Simulation Of $Sin^2\psi$ Diagram in Stress Determination of Textured Materials*, The 2012 International Conference on Green Technology and Sustainable Development, Vietnam, Sep. 2012, pp.201-204.

[4] Lê Chí Cương, *Development of Automated X–ray Stress Analyzer and its Applications in Stress Measurement of Textured Materials*, PhD. Thesis, 2004.

[5] V.Hauk, *Structural and Residual Stress Analysis by Nondestructive Methods*, Elsevier, 1997, pp. 254-298.

[6] V. Hauk, H. Hougardy, E. Macherauch, *Residual Stresses Measurement-Calculation-Evaluation*, Informations Gesellschart, 2005, p.255.

[7] Landolt–Bornstein, *Numerical Data and Functional Relationship in Science and Technology*, New Series, Gruppe III, Vol. 11, Springer Verlag, Berlin, Heidelberg, New York, p.142.

[8] I.C.Noyan, J.B.Cohen, *Residual Stress–Measurement by Diffraction and Interpretation*, Springer–Verlag, 1987, pp.63-72.

[9] Karel Van Acker, *Internal Stress States in Cold Worked Metals and in Metal Matrix Composites*, Katholieke Universiteit Leuven, 2008, pp.33-47.

[10] Keisuke Tanaka, Shotaro Kodama and Toru Goto, *X–ray Diffraction Studies on The Deformation And Fracture of Solids,* Elsevier, Applied Science, pp. 1-27.